Synthetic Molecular Machines Hot Paper

DOI: 10.1002/anie.201403091

Motion Capture and Manipulation of a Single Synthetic Molecular Rotor by Optical Microscopy**

*Tomohiro Ikeda, Takahiro Tsukahara, Ryota Iino, Masayuki Takeuchi, and Hiroyuki Noji**

Abstract: *Single-molecule imaging and manipulation with optical microscopy have become essential methods for studying biomolecular machines; however, only few efforts have been directed towards synthetic molecular machines. Single-molecule optical microscopy was now applied to a synthetic molecular rotor, a double-decker porphyrin (DD). By attaching a magnetic bead (ca. 200 nm) to the DD, its rotational dynamics were captured with a time resolution of 0.5 ms. DD showed rotational diffusion with 90° steps, which is consistent with its four-fold structural symmetry. Kinetic analysis revealed the first-order kinetics of the 90° step with a rate constant of 2.8 s^{-1}. The barrier height of the rotational potential was estimated to be greater than 7.4 kJ mol^{-1} at 298 K. The DD was also forcibly rotated with magnetic tweezers, and again, four stable pausing angles that are separated by 90° were observed. These results demonstrate the potency of single-molecule optical microscopy for the elucidation of elementary properties of synthetic molecular machines.*

Cells employ a large variety of nanometer-sized biomolecular machines, such as F_1-ATPase.[1] Single-molecule imaging and manipulation techniques with optical microscopy have been developed to understand the mechanisms of biomolecular machines.[2] Generally, it requires the attachment of an optically detectable probe, for example, a fluorescent dye (ca. 1 nm in size), a gold colloid (ca. 10–100 nm), a magnetic or a polystyrene bead (ca. 0.1–1 μm), onto the molecule of interest, which is fixed on a glass substrate. The conformational dynamics of individual biomolecular machines can be captured by monitoring the motion of the probe. Furthermore, single-molecule manipulation techniques, such as optical and magnetic tweezers, allow us to investigate how external forces affect a catalytic reaction and to characterize inherently unstable molecular conformations.[2d,3] These approaches for motion capture and manipulation have unveiled the fundamental properties of biomolecular machines, that is, the force, directionality, and energetics of their motions, which cannot be revealed by ensemble measurements.

Biomolecular machines have inspired chemists to create synthetic molecular machines, many of which have already been used as switches[4] and motors.[5] Their conformational changes can be flexibly designed so as to control their functions with stimuli, such as light, heat, acid/base, redox chemistry, or molecular recognition. Conventionally, spectroscopic methods, including NMR, UV/Vis absorption, and circular dichroism spectroscopy, and single-molecule scanning tunneling microscopy (STM)[6] have been utilized to characterize synthetic molecular machines. Furthermore, the force generated by single synthetic molecular machines has been measured by atomic force microscopy.[7] Although such ensemble measurements and single-molecule studies provide information on dynamics, single-molecule optical microscopy should be advantageous when seeking detailed information on the intrinsic kinetics, dynamics, and energetics of synthetic molecular machines.

Herein, we employed single-molecule optical microscopy with a probe (200 nm magnetic bead) to characterize the rotational dynamics of a double-decker porphyrin (DD), which is a 1 nm sized synthetic molecular rotor.[8] Our approach, which entails single-molecule motion capture and manipulation of the synthetic molecular machines, should complement the existing techniques and contribute to unveiling the fundamental properties of such molecular systems.

DD is a 1 nm sized synthetic rotor composed of two porphyrin rings that are connected through a coordinated central metal ion. Evidence for the intramolecular rotation of the porphyrin rings was obtained by spectroscopic analysis[8f–h] and STM studies.[6c–f] These studies suggested that the rotational step size for *meso*-tetraaryl porphyrin-based DD is 90° and that the potential barrier for rotation of DD depends on the ionic radius of the central metal ion and the bulkiness of the substituents on the side chains of the porphyrin rings. Considering the above-mentioned characteristics of DD, we designed and synthesized a cerium bis(porphyrinate) double-

[*] Dr. T. Ikeda, T. Tsukahara, Prof. H. Noji
Department of Applied Chemistry, School of Engineering
The University of Tokyo
Bunkyo-ku, Tokyo 113-8656 (Japan)
E-mail: hnoji@appchem.t.u-tokyo.ac.jp
Prof. H. Noji
Core Research for Evolutional Science and Technology (Japan)
Science and Technology Agency
Sanban-cho, Chiyoda-ku, Tokyo 102-0075 (Japan)
Prof. R. Iino
Okazaki Institute for Integrative Bioscience
Institute for Molecular Science
National Institutes of Natural Sciences
Higashiyama, Myodaijicho, Okazaki, Aichi 444-8787 (Japan)
Prof. M. Takeuchi
Organic Materials Group, Polymer Materials Unit
National Institute for Materials Science
1-2-1 Sengen, Tsukuba, Ibaraki 305-0047 (Japan)

[**] This work was supported by CREST (Core Research for Evolutional Science and Technology) of the Japan Science and Technology Agency and Grant-in-Aids for Scientific Research (18074005 to H.N., 24651167 to R.I., and 21108010 to M.T.) from the Ministry of Education, Science, Sports, and Culture of Japan.

Supporting information for this article is available on the WWW under http://dx.doi.org/10.1002/anie.201403091.

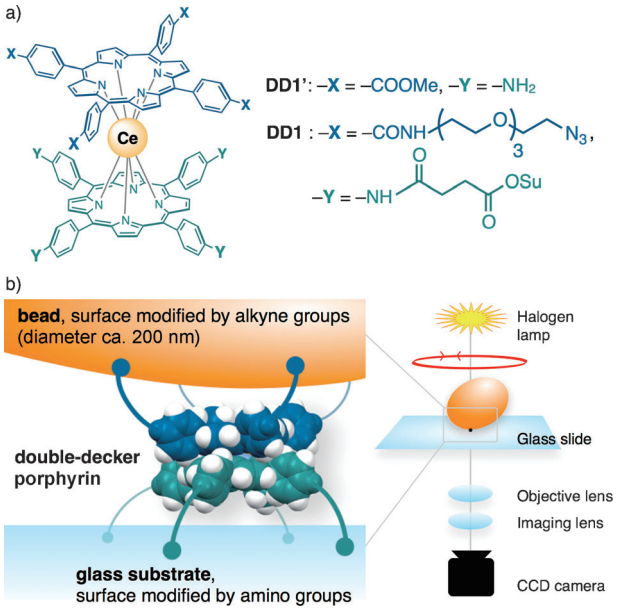

Figure 1. Experimental setup. a) Chemical structure of **DD1**. b) Microscope setup for imaging the rotational dynamics of DD. Su = succinimidyl.

decker species, **DD1′** (Figure 1a; see also the Supporting Information, Scheme S1).[8a]

DD1′ comprises two different porphyrin rings, which were modified with active-ester-terminated succinyl linkers and azide-terminated triethyleneglycol linkers, respectively (**DD1** in Figure 1a; Scheme S2). Therefore, **DD1** can be selectively attached to the surface of an amino-modified glass substrate and an active-alkyne-modified magnetic bead through aminolytic amide bond formation and a catalyst-free click reaction, respectively.

The sample for observation was prepared by sequentially attaching a magnetic bead onto **DD1** on the surface of the cover glass (for details, see the Supporting Information). The rotational dynamics of the bead were visualized with an optical microscope under halogen-lamp illumination. The phase-contrast images were recorded using a CCD camera at 30–2000 frames per second (fps) at room temperature (Figure 1b).

Considering the Lennard–Jones potential, which is highly dependent on the distance between the surfaces of a bead and a substrate, we expected bead and glass to be free from mutual van der Waals interactions because they are separated by a DD with a height of approximately 1 nm. We also used dimethyl sulfoxide (DMSO) as the solvent, expecting a weaker van der Waals interaction in DMSO than in a polar solvent, such as water.[9]

For the cerium ion embedded in DD, two stable redox states, Ce^{IV}DD and Ce^{III}DD, are known. In the presence of amines, light irradiation causes the photochemical reduction from Ce^{IV} to Ce^{III}.[8e] Under the present experimental conditions, where **DD1** anchored on the poly(allylamine)-coated glass was studied under intense irradiation with visible light, the cerium ion of **DD1** was confirmed to be Ce^{III} by control experiments in solution (Figure S4). Solvent exchange experiments monitored by optical microscopy also supported this assumption (see below).

Figure 2a shows an image of the used magnetic beads. Many beads showed rotational diffusion in a random direction, while some were immobile. Among the beads that showed rotational Brownian motion, 13% (14/105) rotated with discrete steps only in the presence of **DD1** (Figure 2b,c; see also Table S1). Most of them showed rotational diffusion with four steps of 90° each (Figure 2d), as expected from the structural four-fold symmetry of **DD1** (Movie S1). Control experiments without DD showed that nonspecifically attached beads were immobile or underwent rotational diffusion without steps (Figure S3 and Movie S2). In our experiments, it was difficult to completely suppress the nonspecific adsorption of the beads onto the glass because of van der Waals interactions. Thus, we concluded that the beads without obvious steps were ones that were nonspecifically bound or that were specifically attached to **DD1** through a single bond, which allows free rotation. Consistent with this hypothesis, switches between rotations with and without steps have not been observed.

All experiments except for the single-molecule manipulation experiment were performed without magnetic tweezers (see below). If the bead rotates in a stepwise manner when

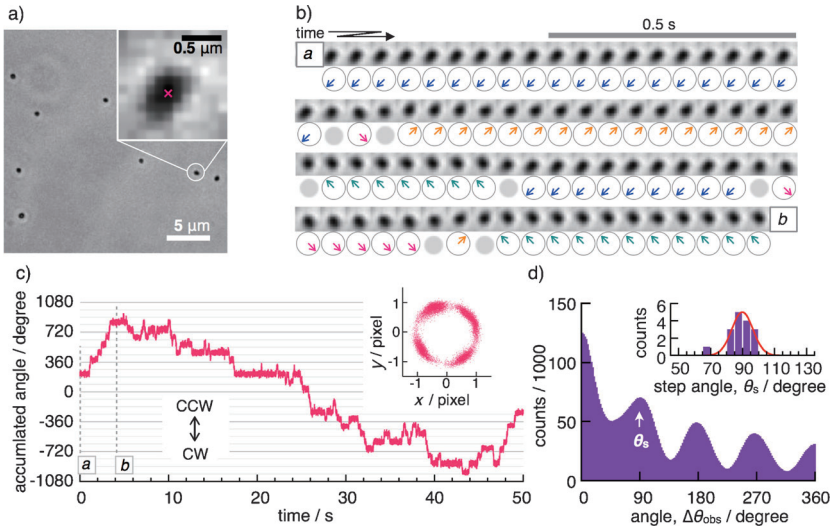

Figure 2. Typical results for the single-molecule imaging of the rotation of **DD1**. a) Wide-field and magnified image (inset) of the beads (111 nm/pixel). The red cross indicates the centroid of the bead. b) Sequential images of a bead recorded at 2000 fps (images linearly averaged to 20 fps). The arrows in the circles indicate the orientation of the bead. The time points "*a*" and "*b*" correspond to those in Figure 2c. c) Time course of the rotation. A positive change in the accumulated angle corresponds to a CCW rotation. The inset shows the *xy* trajectory of the bead centroid. d) Pairwise angle analysis of the time course. The arrow indicates the step size of the bead. Inset: step-size distribution for 16 beads.

magnetized by the apparatus, the pauses must appear at the same four angles for all beads. However, this was not the case. Therefore, the stepping motion of the magnetic bead is not due to the external magnetic field. For this analysis, we only employed the beads that rotated in 90° steps.

To corroborate that the observed stepping motion represented the motion of **DD1**, ferrocenium hexafluorophosphate ($FcPF_6$, 15 mM) in DMSO was injected into the flow chamber to oxidize coordinated Ce^{III} to Ce^{IV} ions (Figure S4). As Ce^{IV} has a smaller ionic radius than Ce^{III} (0.97 Å vs. 1.14 Å),[8e–f] the steric interaction of the two porphyrin rings will be larger in the **DD1** that embeds a Ce^{IV} ion, **DD1-iv**, than in the **DD1** that embeds a Ce^{III} ion, **DD1-iii**, thus interfering with the rotation. Several angle histograms that were obtained before and after infusion of the $FcPF_6$ containing medium are shown in Figure 3. After oxidation, all of the beads (beads I–III in Figure 3 and in Movie S4) stopped to show stepwise rotational diffusion. On the other hand, nonspecifically attached beads did not respond to $FcPF_6$ infusion in the absence of **DD1** (bead IV in Figure 3). We have not observed re-reduced molecules (Ce^{IV} to Ce^{III}) because the beads were detached from the glass by flow during the repeated solvent exchange.

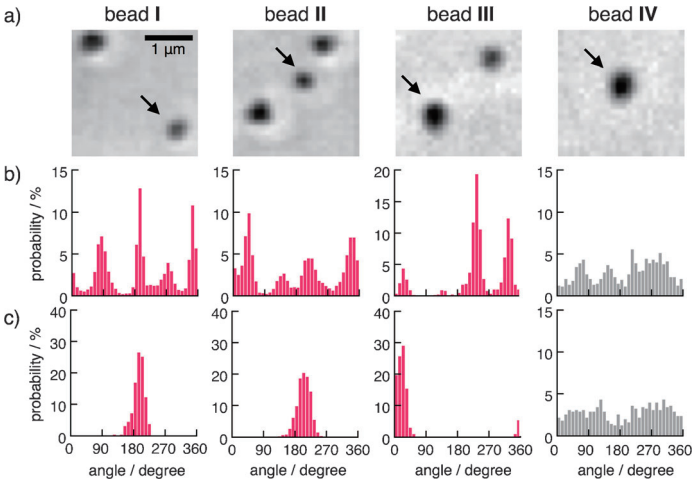

Figure 3. Solvent-exchange experiment to oxidize the cerium ion coordinated to DD. a) Images of the beads shown in Movie S4. Beads I–III exhibited rotational diffusion with 90° steps before oxidation. Bead IV represents the rotation of a nonspecifically bound bead in the absence of DD. b,c) Angle histograms of the individual molecules before (b) and after (c) the addition of the oxidant, $FcPF_6$.

The kinetics of the rotational diffusion of **DD1-iii** were assessed by measuring the dwell times of the pauses between the 90° steps. The pauses before clockwise (CW) and counterclockwise (CCW) steps were analyzed together (Figure 4a). A typical dwell-time histogram obtained from a **DD1-iii** molecule is shown in Figure 4b. The distribution showed an exponential decay. Thus, the 90° step rotation by **DD1-iii** has a single kinetic bottleneck, that is, the rotation is a first-order reaction. We calculated the average rate constant (k_s) of the reaction as $2.8 \pm 0.4\ s^{-1}$ (mean ± SD counted for 16 beads), which corresponds to a half-life of 0.25 ± 0.04 s (Figures S5

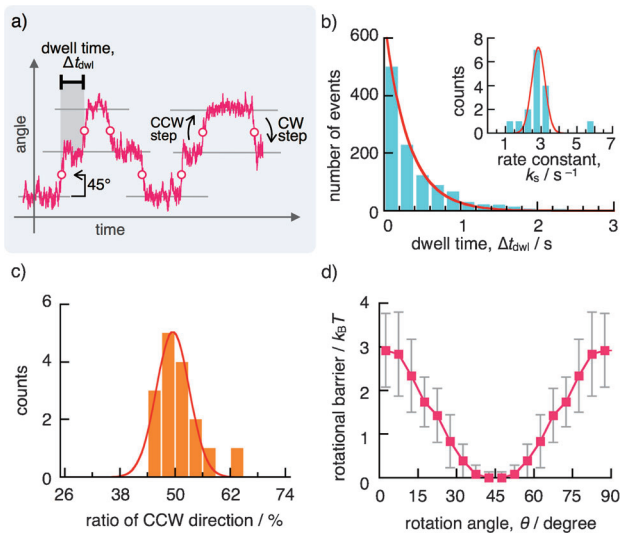

Figure 4. Kinetic analysis of the 90° steps and the rotational potential of **DD1**. a) Determination of the dwell time for the pauses between the 90° steps. b) Histogram of the dwell times for a single bead. The solid line shows the fit to the exponential decay function; $A \times e^{(-k_s t)}$, where k_s is the rate constant of a 90° step. Inset: histogram of k_s for 16 beads. c) Histogram for the ratio of the CCW 90° steps. The ratio was estimated for each bead by counting the number of CW and CCW steps. The movies recorded for 16 beads (30 s each) were analyzed. d) Rotational potential of the beads. The potential was estimated from the angle histogram according to the Boltzmann distribution; $E_i/k_B T = -\ln P_i$, where E_i, k_B, T, and P_i are the energy of the angle i, the Boltzmann constant, the temperature, and the probability that the bead is oriented at an angle i, respectively.

and S6 and Movie S3). The observed rate constant is evidently smaller than the expected time constant assuming that for **DD1-iii**, the steps occur with a similar rate to DD coordinated to La^{III} (ca. $100\ s^{-1}$).[8f] This is attributable to the viscous friction of the magnetic beads attached on **DD1-iii**. We also analyzed the directionality of the steps by counting the number of CW and CCW steps. The probabilities were the same for the two directions (50 ± 4 %, mean ± SD counted for 16 beads; Figure 4c). Therefore, the observed rotation corresponds to random Brownian diffusion with 90° steps.

Evidently, the kinetic bottleneck is the rotational diffusion over the potential barrier between the pausing positions. To estimate the energetic barrier for the 90° steps, we analyzed the probability density of the angular positions of the beads. We used a time resolution of 0.5 ms, which is sufficiently fast to capture the motion of a 200 nm bead (Figure S7),[10] and then determined the potential shape of the rotation-angle distribution of **DD1-iii** according to the Boltzmann distribution (Figure 4d). The potential basin was approximated to be harmonic with a spring constant of $85\ pN\,nm\,rad^{-2}$. The torque as the maximum slope of the potential is $33\ pN\,nm\,rad^{-1}$, and the activation energy for a 90° step was determined to be $3 k_B T$ ($7.4\ kJ\,mol^{-1}$). This value may be the lower limit of the activation energy for a 90° step, because the flexible linkers of **DD1-iii** can attenuate the potential shape.

Next, we forcibly rotated the bead attached to **DD1-iii** with magnetic tweezers (Figure 5a).[2d] The stiffness of the magnetic tweezers was set to approximately $220\ pN\,nm\,rad^{-2}$.

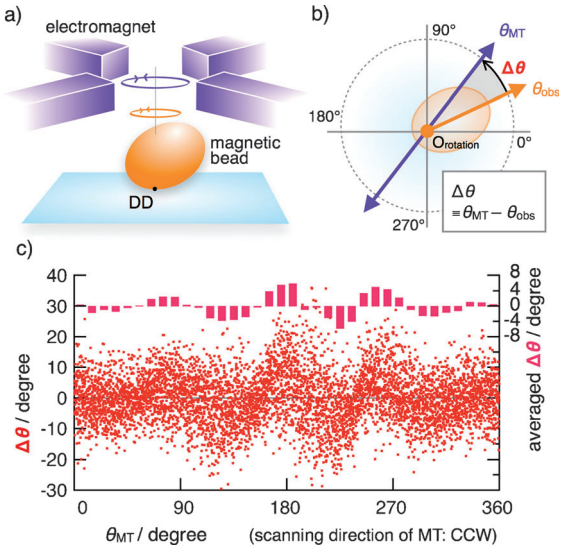

Figure 5. Single-molecule manipulation with magnetic tweezers. a) Experimental setup. b) Angle deviation ($\Delta\theta$) between the magnetic beads (θ_{obs}) and the external magnetic field (θ_{MT}). c) Plots of $\Delta\theta$ (red dots) and its average (pink bars in the top).

The bead orientation was determined by the balance of the torques between the magnetic tweezers and **DD1-iii** (Figure 5b). When the magnetic field was rotated CCW at 0.02 Hz, a periodical response of the bead was observed; the bead increased and decreased its rotational velocity four times per turn. This is evident when the angle deviation ($\Delta\theta$) of the magnetic bead (θ_{obs}) from the magnetic field orientation (θ_{MT}) is plotted against θ_{MT} (Figure 5c). Such a result is reasonable when we consider that **DD1-iii** has a four-fold symmetric rotational potential; it pushes or pulls the bead when the bead is on the downward slope or on the upward slope, respectively. Thus, we detected the four-fold rotational potential of **DD1-iii** by both passive observation and active manipulation.

In summary, we have successfully captured the intramolecular rotation of **DD1** at the single-molecule level using optical microscopy and a relatively large probe. Our techniques will open the way for unveiling fundamental properties of synthetic molecular machines, for example, stepwise motion, potential shapes, and the force or torque that the molecule exerts, which cannot be resolved by ensemble-molecule measurements. We expect that many artificial molecular motors, which have been synthesized already or will be designed in the future, could be characterized by this method.

Received: March 7, 2014
Revised: May 9, 2014
Published online: ■■ ■■, ■■■■

Keywords: molecular dynamics · molecular machines · optical microscopy · single-molecule studies · porphyrins

[1] a) H. Noji, R. Yasuda, M. Yoshida, K. Kinosita, *Nature* **1997**, *386*, 299–302; b) D. Okuno, R. Iino, H. Noji, *J. Biochem.* **2011**, *149*, 655–664; c) R. D. Vale, R. A. Milligan, *Science* **2000**, *288*, 88–95.

[2] a) A. Yildiz, M. Tomishige, A. Gennerich, R. D. Vale, *Cell* **2008**, *134*, 1030–1041; b) M. H. Larson, W. J. Greenleaf, R. Landick, S. M. Block, *Cell* **2008**, *132*, 971–982; c) K. Fujita, M. Iwaki, A. H. Iwane, L. Marcucci, T. Yanagida, *Nat. Commun.* **2012**, *3*, 956; d) R. Watanabe, D. Okuno, S. Sakakihara, K. Shimabukuro, R. Iino, M. Yoshida, H. Noji, *Nat. Chem. Biol.* **2012**, *8*, 86–92.

[3] V. Egger, K. Svoboda, Z. F. Mainen, *J. Neurosci.* **2003**, *23*, 7551–7558.

[4] a) E. R. Kay, D. A. Leigh, F. Zerbetto, *Angew. Chem.* **2007**, *119*, 72–196; *Angew. Chem. Int. Ed.* **2007**, *46*, 72–191; b) G. S. Kottas, L. I. Clarke, D. Horinek, J. Michl, *Chem. Rev.* **2005**, *105*, 1281–1376.

[5] a) T. R. Kelly, R. A. Silva, H. De Silva, S. Jasmin, Y. J. Zhao, *J. Am. Chem. Soc.* **2000**, *122*, 6935–6949; b) T. R. Kelly, H. De Silva, R. A. Silva, *Nature* **1999**, *401*, 150–152; c) N. Koumura, R. W. Zijlstra, R. A. van Delden, N. Harada, B. L. Feringa, *Nature* **1999**, *401*, 152–155; d) N. Koumura, E. M. Geertsema, M. B. van Gelder, A. Meetsma, B. L. Feringa, *J. Am. Chem. Soc.* **2002**, *124*, 5037–5051; e) D. A. Leigh, J. K. Y. Wong, F. Dehez, F. Zerbetto, *Nature* **2003**, *424*, 174–179; f) J. V. Hernandez, E. R. Kay, D. A. Leigh, *Science* **2004**, *306*, 1532–1537.

[6] a) M. Alemani, M. V. Peters, S. Hecht, K. H. Rieder, F. Moresco, L. Grill, *J. Am. Chem. Soc.* **2006**, *128*, 14446–14447; b) T. Kudernac, N. Ruangsupapichat, M. Parschau, B. Macia, N. Katsonis, S. R. Harutyunyan, K. H. Ernst, B. L. Feringa, *Nature* **2011**, *479*, 208–211; c) H. Tanaka, T. Ikeda, M. Takeuchi, K. Sada, S. Shinkai, T. Kawai, *ACS Nano* **2011**, *5*, 9575–9582; d) J. Otsuki, S. Kawaguchi, T. Yamakawa, M. Asakawa, K. Miyake, *Langmuir* **2006**, *22*, 5708–5715; e) J. Otsuki, M. Taka, D. Kobayashi, *Chem. Lett.* **2011**, *40*, 717–719; f) J. Otsuki, Y. Komatsu, D. Kobayashi, M. Asakawa, K. Miyake, *J. Am. Chem. Soc.* **2010**, *132*, 6870–6871; g) D. Lensen, J. A. A. W. Elemans, *Soft Matter* **2012**, *8*, 9053–9063; h) D. Écija, W. Auwarter, S. Vijayaraghavan, K. Seufert, F. Bischoff, K. Tashiro, J. V. Barth, *Angew. Chem.* **2011**, *123*, 3958–3963; *Angew. Chem. Int. Ed.* **2011**, *50*, 3872–3877; i) H. L. Tierney, C. J. Murphy, A. D. Jewell, A. E. Baber, E. V. Iski, H. Y. Khodaverdian, A. F. McGuire, N. Klebanov, E. C. H. Sykes, *Nat. Nanotechnol.* **2011**, *6*, 625–629; j) U. G. E. Perera, F. Ample, H. Kersell, Y. Zhang, G. Vives, J. Echeverria, M. Grisolia, G. Rapenne, C. Joachim, S. W. Hla, *Nat. Nanotechnol.* **2013**, *8*, 46–51.

[7] a) P. Lussis, T. Svaldo-Lanero, A. Bertocco, C. A. Fustin, D. A. Leigh, A. S. Duwez, *Nat. Nanotechnol.* **2011**, *6*, 553–557; b) A. Van Quaethem, P. Lussis, D. A. Leigh, A. S. Duwez, C. A. Fustin, *Chem. Sci.* **2014**, *5*, 1449–1452.

[8] a) J. W. Buchler, M. Nawra, *Inorg. Chem.* **1994**, *33*, 2830–2837; b) K. Tashiro, T. Fujiwara, K. Konishi, T. Aida, *Chem. Commun.* **1998**, 1121–1122; c) M. Ikeda, M. Takeuchi, S. Shinkai, F. Tani, Y. Naruta, S. Sakamoto, K. Yamaguchi, *Chem. Eur. J.* **2002**, *8*, 5541–5550; d) S. Ogi, T. Ikeda, R. Wakabayashi, S. Shinkai, M. Takeuchi, *Chem. Eur. J.* **2010**, *16*, 8285–8290; e) K. Tashiro, K. Konishi, T. Aida, *J. Am. Chem. Soc.* **2000**, *122*, 7921–7926; f) M. Ikeda, M. Takeuchi, S. Shinkai, F. Tani, Y. Naruta, *Bull. Chem. Soc. Jpn.* **2001**, *74*, 739–746; g) K. Tashiro, K. Konishi, T. Aida, *Angew. Chem.* **1997**, *109*, 882–884; *Angew. Chem. Int. Ed. Engl.* **1997**, *36*, 856–858; h) M. Takeuchi, T. Imada, M. Ikeda, S. Shinkai, *Tetrahedron Lett.* **1998**, *39*, 7897–7900.

[9] L. X. Yang, C. Adam, G. S. Nichol, S. L. Cockroft, *Nat. Chem.* **2013**, *5*, 1006–1010.

[10] D. Okuno, R. Iino, H. Noji, *Eur. Biophys. J. Biophys. Lett.* **2010**, *39*, 1589–1596.

Communications

Synthetic Molecular Machines

T. Ikeda, T. Tsukahara, R. Iino,
M. Takeuchi, H. Noji* ——— ■■■■–■■■■

Motion Capture and Manipulation of a Single Synthetic Molecular Rotor by Optical Microscopy

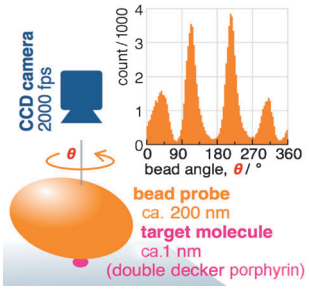

Single-molecule optical microscopy was applied to study the rotation of a double-decker porphyrin. With a magnetic bead as the probe, the rotary diffusion of this synthetic nanorotor with 90° steps was visualized; it is consistent with the four-fold structural symmetry of this molecule.